Relating Out-of-Time-Order Correlations to Entanglement via Multiple-Quantum Coherences

Martin Gärttner,[1,2,*] Philipp Hauke,[2,3,4] and Ana Maria Rey[1]
[1]JILA, NIST, and the University of Colorado, Boulder, Colorado 80309, USA
[2]Kirchhoff-Institut für Physik, Universität Heidelberg, Im Neuenheimer Feld 227, 69120 Heidelberg, Germany
[3]Institute for Theoretical Physics, University of Innsbruck, 6020 Innsbruck, Austria
[4]Institute for Quantum Optics and Quantum Information of the Austrian Academy of Sciences, 6020 Innsbruck, Austria

(Received 7 June 2017; revised manuscript received 14 September 2017; published 24 January 2018)

Out-of-time-order correlations (OTOCs) characterize the scrambling, or delocalization, of quantum information over all the degrees of freedom of a system and thus have been proposed as a proxy for chaos in quantum systems. Recent experimental progress in measuring OTOCs calls for a more thorough understanding of how these quantities characterize complex quantum systems, most importantly in terms of the buildup of entanglement. Although a connection between OTOCs and entanglement entropy has been derived, the latter only quantifies entanglement in pure systems and is hard to access experimentally. In this work, we formally demonstrate that the multiple-quantum coherence spectra, a specific family of OTOCs well known in NMR, can be used as an entanglement witness and as a direct probe of multiparticle entanglement. Our results open a path to experimentally testing the fascinating idea that entanglement is the underlying glue that links thermodynamics, statistical mechanics, and quantum gravity.

DOI: 10.1103/PhysRevLett.120.040402

Entanglement in quantum systems is a resource for quantum computation and communication and has been called *the* characteristic trait of quantum mechanics [1]. Recently, it has also been proposed [2] and experimentally tested in proof-of-principle experiments [3,4] that quantum entanglement is in fact the key concept behind thermalization in isolated quantum systems. Essentially, the approach to equilibrium can be understood as the spreading of entanglement through the system's degrees of freedom. In parallel, the concept of "scrambling" in many-body systems, which refers to the delocalization of quantum information over all of a system's degrees of freedom, has gained great attention [5–13], motivated by the finding that special models with thermal states "holographically dual" to black holes can thermalize and scramble quantum information at the fastest rate allowed by nature [14,15]. The scrambling rate can be quantified through out-of-time-ordered correlators (OTOCs), which have been connected to entanglement via the Rényi entropy [5,16]. However, the Rényi entropy is a strict entanglement monotone only for pure systems and hard to access experimentally, requiring resources that scale exponentially with the subsystem size as well as single-particle addressing. Therefore, it is desirable to establish experimentally accessible entanglement witnesses applicable to open as well as isolated quantum systems, which can be used to quantify scrambling.

In this Letter, we formally show that a specific family of OTOCs, first developed in NMR under the name of the multiple-quantum coherence (MQC) spectra, are useful entanglement witnesses. The MQC protocol has been known for many years to be a suitable method to quantify the development of many-body quantum coherences [17,18]. Recently, it has been applied to describe the spreading of correlations [17,19–21] and as a signature of localization effects [22–25]. While connections between MQCs and entanglement have been pointed out in Refs. [26–28] and witnesses of two-particle entanglement have been constructed in Refs. [29,30], to date a formal relation between the MQC spectrum and multiparticle entanglement generally applicable to mixed states does not exist. Here, we formally establish such a relation by deriving entanglement witnesses from the MQC intensities, as well as a relationship between MQCs and the quantum Fisher information (QFI) [31,32], a well-known witness of multiparticle entanglement.

To illustrate the power of these connections, we use the specific example of a long-range Ising model in a transverse field. We start the dynamics from a pure initial state, but show the applicability of the witness to mixed states by including decoherence arising from light scattering during the dynamics. This type of decoherence is relevant for a broad class of quantum systems. Our results demonstrate the existence of an experimentally accessible link between scrambling measured by OTOCs and entanglement, provided by the MQCs.

MQCs have a long tradition in NMR systems, which typically operate at high temperature. Measuring MQCs in pure and almost zero temperature initial states is now becoming feasible in cold-atom experiments, including

Bose-Einstein condensates, ultracold atoms in cavities, or trapped ions [7,33–39]. Such experiments open the possibility to probe the rich information contained in an entangled state via MQCs.

We start by introducing the MQCs, which have been used as a means for quantifying quantum coherence [17,18,20]. Let $|\psi_i\rangle$ be the eigenstates of a Hermitian operator $\hat{A}$ and λ_i the corresponding discrete eigenvalues. We divide the density matrix of an arbitrary state $\hat{\rho}$ into blocks as $\hat{\rho} = \sum_m \sum_{\lambda_i-\lambda_j=m} \rho_{ij}|\psi_i\rangle\langle\psi_j| = \sum_m \hat{\rho}_m$. Thus, $\hat{\rho}_m$ contains all coherences between states with eigenvalues of $\hat{A}$ that differ by m. An experimentally accessible quantifier of these MQCs is the Frobenius norm $I_m(\hat{\rho}) = (\|\hat{\rho}_m\|_2)^2 = \mathrm{tr}[\hat{\rho}_m^\dagger \hat{\rho}_m]$ called multiple-quantum intensity. The key idea is that I_m can be directly accessed in an experiment that has the ability to reverse the dynamics that created the state of interest $\hat{\rho}$ from an initial fiducial state $\hat{\rho}_0$. In this context, the time reversal can be connected with the concept of many-body Loschmidt echoes, well-known probes of irreversibility and chaos [40–44].

The protocol to measure I_m is [17,39] (see Fig. 1) as follows: evolve $\hat{\rho}_0$ into $\hat{\rho}_t$ under a nontrivial unitary evolution $e^{-i\hat{H}_{\mathrm{int}}t}$, apply $\hat{W}(\phi) = e^{-i\hat{A}\phi}$, evolve backward with $e^{i\hat{H}_{\mathrm{int}}t}$ to $\hat{\rho}_f$, and finally measure the probability to find the system in the initial state $\mathrm{tr}[\hat{\rho}_0\hat{\rho}_f]$ (if $\hat{\rho}_0$ is pure, this is the fidelity). Noting that $\hat{W}(\phi)\hat{\rho}_m\hat{W}^\dagger(\phi) = e^{im\phi}\hat{\rho}_m$ and using cyclic permutations under the trace, one finds

$$F_t(\phi) \equiv \mathrm{tr}[\hat{\rho}_0\hat{\rho}_f] = \mathrm{tr}[\hat{\rho}_t\hat{\rho}_t(\phi)] = \sum_m I_m(\hat{\rho}_t)e^{-im\phi}, \quad (1)$$

where $\hat{\rho}_t(\phi) = \hat{W}(\phi)\hat{\rho}_t\hat{W}^\dagger(\phi)$. Thus, by Fourier transforming the signal with respect to ϕ, one obtains the MQC spectrum $\{I_m(\hat{\rho}_t)\}$ (see [45] for details). For NMR systems typically operating at infinite temperature, this overlap measurement reduces to a magnetization measurement, making it possible to observe coherences as high as $m \sim 7000$ [23,24]. Nevertheless, the perturbative nature of the coherences present in highly mixed states, which facilitates experimental access of the MQCs, also implies that the underlying quantum complexity and entanglement content in those states are small in comparison to pure states. For pure states, measuring MQCs requires a fidelity measurement that encodes information about N-body correlations in an N-particle system [59]. Despite the fact that, in general, the resources required for measuring fidelity scale unfavorably with the system size, the feasibility of such a measurement has been demonstrated for up to 50 particles [39], much beyond what is possible with schemes involving measuring entanglement entropy.

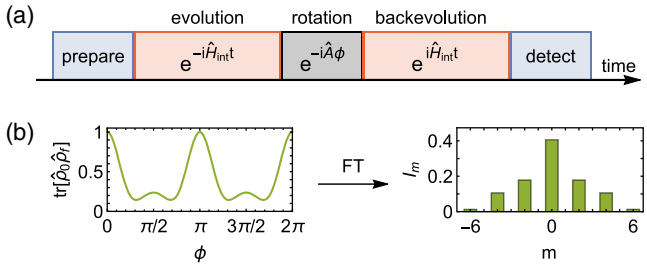

FIG. 1. (a) Illustration of the scheme for measuring the coherences using time reversal. The state of interest $\hat{\rho}_t$ is reached after the first evolution period. The rotation then imprints a phase $m\phi$ on each sector $\hat{\rho}_m$ of the density matrix (see text). Evolving backward and measuring the overlap with the initial state as a function of ϕ, the coherences I_m of $\hat{\rho}_t$ are retrieved as the Fourier components of this signal. (b) An example for the fidelity signal obtained from time evolution under the Ising Hamiltonian [Eq. (5) with $\Omega = 0$] and rotations about the z axis of the spin ($\hat{A} = \hat{S}_z$). By Fourier transforming this signal, one obtains the intensities I_m, which quantify the magnitude of the mth order coherences of $\hat{\rho}_t$.

The connection between MQCs and OTOCs becomes apparent from $\hat{\rho}_t = e^{-i\hat{H}_{\mathrm{int}}t}\hat{\rho}_0 e^{i\hat{H}_{\mathrm{int}}t}$. By defining $\hat{V}_0 = \hat{\rho}_0$, if $\hat{V}_0\hat{\rho}_0 = \hat{\rho}_0$ [60], the above expression can be recast as [25,39]

$$\begin{aligned} F_t(\phi) &\equiv \mathrm{tr}[\hat{W}_t^\dagger(\phi)\hat{V}_0^\dagger\hat{W}_t(\phi)\hat{V}_0\rho_0] \\ &= \langle W_t^\dagger(\phi)\hat{V}_0^\dagger\hat{W}_t(\phi)\hat{V}_0\rangle, \end{aligned} \quad (2)$$

where $\hat{W}_t(\phi) = e^{i\hat{H}_{\mathrm{int}}t}\hat{W}(\phi)e^{-i\hat{H}_{\mathrm{int}}t}$. $F_t(\phi)$ is therefore an OTOC function, a specific product of Heisenberg operators not acting in normal order. When $\hat{W}(\phi)$ and $\hat{V}_0$ are chosen to be initially commuting operators, then $F_t(\phi) = 1 - \langle|[\hat{W}_t(\phi), \hat{V}_0]|^2\rangle$. The growth of the norm of the commutator, i.e., the degree by which the initially commuting operators fail to commute at later times due to the many-body interactions generated by $\hat{H}_{\mathrm{int}}$, is commonly used as an operational definition of the scrambling rate [5–7]. Scrambling can be interpreted as the process by which the information encoded in the initial state, through the interactions, is distributed over the other degrees of freedom of the system. This process makes it no longer possible to retrieve the initial information by local operations and measurements.

We are now in the position to state the main results of the Letter.

First, the second moment of the MQC spectrum [$F_I/2$, defined in Eq. (3)] provides a lower bound on the quantum Fisher information F_Q

$$\begin{aligned} F_I(\hat{\rho}_t, \hat{A}) &\equiv 2\sum_{m=-N}^{N} I_m(\hat{\rho}_t)m^2 \\ &= -2\frac{\partial^2 F_t(\phi)}{\partial\phi^2}\bigg|_{\phi=0} \le F_Q(\hat{\rho}_t, \hat{A}). \end{aligned} \quad (3)$$

This expression becomes an equality for pure states $\hat{\rho}_t$.

The QFI has been introduced to quantify the maximal precision with which a parameter ϕ in the unitary

$\hat{W}(\phi) = e^{-i\hat{A}\phi}$ can be estimated using the quantum state $\hat{\rho}$ as an input to an interferometer. It bounds the minimal variance of ϕ as $\Delta\phi \geq 1/\sqrt{F_Q(\hat{\rho}, \hat{A})}$ (Cramér-Rao bound) [61]. It has been shown that, if $F_Q(\hat{\rho}, \hat{A}) > b_k \equiv nk^2 + (N - nk)^2$ where n is the integer part of N/k, then $\hat{\rho}$ is $(k+1)$-particle entangled [62–64]. To derive expression (3), we used the relation $F_I(\hat{\rho}, \hat{A}) = 4\mathrm{tr}[\hat{\rho}^2\hat{A}^2 - (\hat{\rho}\,\hat{A})^2]$, which is a lower bound on the QFI [65] (see also [45]). The choice of the generator $\hat{A}$ can be optimized for detecting the entanglement of a given state using intuition from quantum metrology.

The relation (3) has a number of implications, the most direct one being that F_I inherits the property of F_Q of being a witness for multiparticle entanglement; i.e., $F_I > b_k$ implies $F_Q > b_k$ and thus $(k+1)$-particle entanglement. This allows us to establish an intimate connection between scrambling of quantum information and the buildup of entanglement. Namely, the ϕ dependence of the OTOC $F_t(\phi)$ encodes information about the entanglement content of the state $\hat{\rho}_t$. We also note that, for thermal states, QFI can be directly related to dynamic susceptibilities, as demonstrated in Refs. [66] [see explicitly Eq. (4)] and [67], which are well-known signatures of quantum critical behavior and phase transitions. Moreover, the QFI is a measure of macroscopic coherences, such as appear in "cat states" [65].

Second, each individual I_m by itself can be used as an entanglement witness. The quantity F_I only characterizes the second moment of the MQC spectrum or, equivalently, only depends on the small-ϕ behavior of the measured observable $F_t(\phi)$, while the MQC spectrum, i.e., each individual I_m, contains much more detailed information about the state $\hat{\rho}$. To show that individual I_m can witness entanglement, we use two properties [45]: First, the I_m are convex, or nonincreasing, under mixing $[I_m[p\hat{\rho}_1 + (1-p)\hat{\rho}_2] \leq pI_m(\hat{\rho}_1) + (1-p)I_m(\hat{\rho}_2)$ for $m \neq 0]$. Second, coherences of product states can be obtained from those of the constituent subensembles by $I_m(\hat{\rho}_A \otimes \hat{\rho}_B) = \sum_k I_{m+k}(\hat{\rho}_A)I_{m-k}(\hat{\rho}_B)$. With these two properties, one can, for a given m, bound the maximal I_m achievable on the set of separable states.

In the following, we outline how to derive such bounds for systems of spin 1/2 particles. The detailed proof can be found in the Supplemental Material [45]. The spins are described by Pauli operators $\hat{\sigma}_j^\alpha$, $\alpha = x, y, z$, $j = 1, \ldots, N$, with the eigenstates of $\hat{\sigma}_j^z$ denoted by $|\uparrow\rangle_j$ and $|\downarrow\rangle_j$. We calculate the maximal I_m achievable with a separable state. Without loss of generality, we choose $\hat{A} = \hat{S}_z = \sum_j \hat{\sigma}_j^z/2$ [68]. It follows from the convexity that the maximum I_m is assumed for pure states, which for separable states take the most general form $\bigotimes_j(\sqrt{p_j}|\uparrow\rangle_j + e^{i\varphi_j}\sqrt{1-p_j}|\downarrow\rangle_j)$. From the rule for building tensor products, it follows that I_m is independent of φ_j and is a quadratic polynomial in the p_j. Noting that I_m is invariant under $p_j \to 1 - p_j$, the maximum is assumed when all p_j are either extremal (zero or one) or equal to 1/2. For such a state with N_+ spins in the equal superposition state ($p = 1/2$), I_m can be calculated analytically and optimized numerically with respect to N_+, which yields

$$I_m^{\mathrm{max,sep}} = \max_{N_+ \in \{0,\ldots,N\}} \frac{(2N_+)!}{4^{N_+}(N_+ - m)!(N_+ + m)!}. \quad (4)$$

Thus, if for a given state $\hat{\rho}$ and rotation generated by $\hat{A}$, one has $I_m > I_m^{\mathrm{max,sep}}$ for some m, then $\hat{\rho}$ must be entangled. Note also that I_N is a witness of genuine N-partite entanglement [69].

We now illustrate these results by applying them to the specific case of collective spin models. We consider a system of N spin 1/2 particles and the coherences with respect to the collective spin operator $\hat{A} = \hat{S}_{\mathbf{n}} = \sum_j \hat{\mathbf{s}}_j \cdot \mathbf{n}$, with $\hat{\mathbf{s}}_j = (\hat{\sigma}_j^x, \hat{\sigma}_j^y, \hat{\sigma}_j^z)/2$ and a unit vector $\mathbf{n} = (n^x, n^y, n^z)$. Thus, the spectrum of $\hat{A}$ consists of the (half) integers $M = -N/2, \ldots, N/2$, and we define the mth order coherence $\hat{\rho}_m$ as the block of the density matrix spanned by $|\phi_M\rangle\langle\phi_{M+m}|$, where $|\phi_M\rangle$ are the eigenstates of $\hat{A}$ with eigenvalue M. We study an all-to-all transverse-field Ising model

$$\hat{H}_{\mathrm{int}} = -J/N\hat{S}_x^2 - \Omega\hat{S}_z, \quad (5)$$

where the spins are initially prepared in $|\psi_0\rangle = |\uparrow\rangle^{\otimes N}$. In the absence of decoherence, the dynamics is restricted to the symmetric Dicke manifold, which makes it very easy to numerically simulate the dynamics of large numbers of spins.

In Fig. 2, we illustrate the time evolution of the coherence spectrum I_m for zero and nonzero transverse field. The QFI per particle, shown as a black line, is proportional to the variance of the coherence spectrum. The figure shows that the I_m surpass the bounds for separable states in large parts of the spectrum. A complex pattern of self-interference emerges as soon as the coherences become distributed across the entire spectrum and the initially Gaussian state completely delocalizes in spin space. The two snapshots on the right show a relatively short evolution time, where $\hat{\rho}_t$ is a spin-squeezed near-Gaussian state, and a longer time, where the state becomes clearly non-Gaussian and the I_m develop an intricate structure for both the pure Ising and the transverse-field Ising case. This snapshot corresponds to the longest time that has been measured experimentally for these parameters in [39]. At this time, the I_m fall off at most linearly with m, while the bound decreases exponentially [cf. Eq. (4)]. This means that the degree $(I_m/I_m^{\mathrm{max,sep}})$ to which the entanglement bound is violated increases exponentially with m.

Next, we discuss the impact of decoherence for an example relevant to recent trapped-ion experiments [39,70]. We find that decoherence can substantially reduce

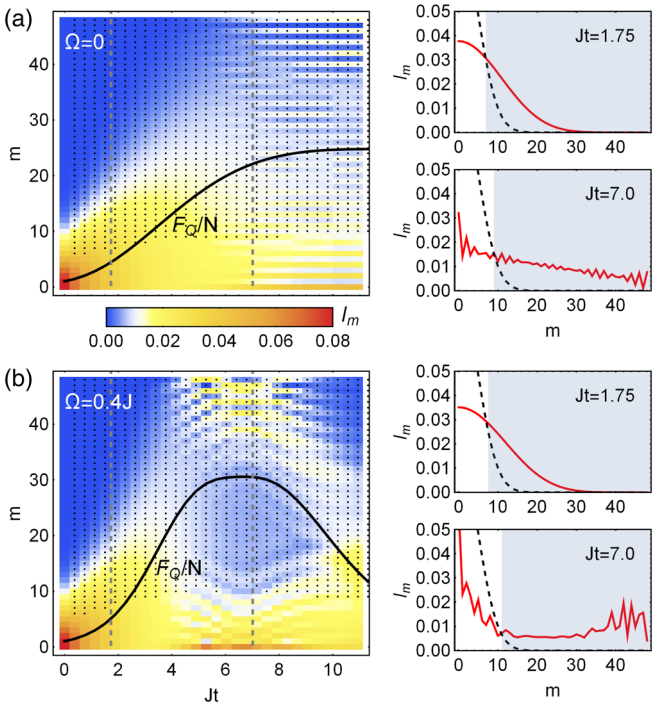

FIG. 2. MQC spectra for evolution under the Ising (a) and transverse-field Ising (b) Hamiltonian as a function of the evolution time for $N = 48$ spins. The QFI per particle is shown on top of the density plot as a solid line. $(k+1)$-particle entanglement is detected if $F_Q/N > b_k/N$ and, in the pure case, $F_Q = F_I$. The direction of the rotation axis $\mathbf{n}$ is optimized for each t. The pixels corresponding to those I_m that violate the bound for separable states are marked with a dot. At late times reflection at the boundary of the MQC spectrum at $m = N$ leads to self-interference and fragmentation of the coherence spectrum. (Right) The coherence spectrum (red solid) and entanglement bounds (black dashed) at specific times, indicated by the dashed lines (left). The gray shading shows for which m the bounds are violated.

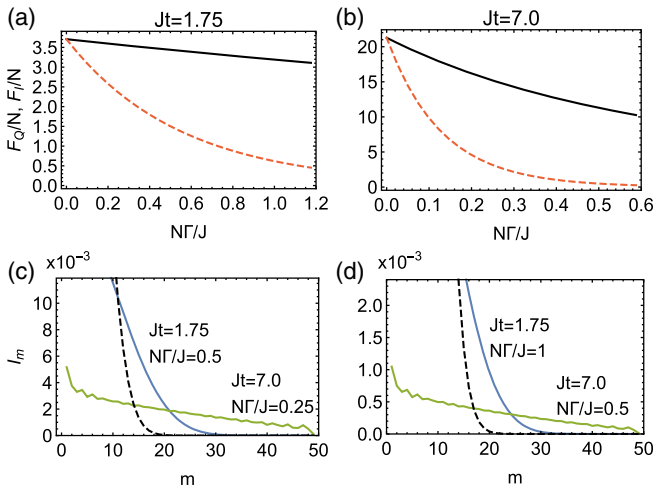

FIG. 3. (a),(b) Optimal QFI (black) and the lower bound $F_I(t)$ (red dashed) as a function of the total decoherence rate $\Gamma = (\Gamma_{ud} + \Gamma_{du} + \Gamma_{el})/2$, scaled by J/N, and pure Ising dynamics ($\Omega = 0$). The relative size of the individual decoherence rates for spontaneous emission and elastic scattering have been chosen $\Gamma_{ud}:\Gamma_{du}:\Gamma_{el} = 1:1:10$. In the pure case ($\Gamma = 0$), the bound coincides with the actual QFI. $F_I(\hat{\rho}_t, \hat{A})$ decays as $\exp[-N\Gamma t]$, much faster than the QFI. The parameter choices are motivated by the parameters of Ref. [39], which corresponds to typical values of (a) $J = 2.9$ kHz and $t = 0.6$ ms and (b) $J = 5.8$ kHz and $t = 1.2$ ms. $N = 48$ spins have been used. (c),(d) Coherences I_m for two different dephasing rates in each case. Increasing the incoherent processes by a factor of 2 [comparing (c) with (d)], the coherences globally decrease, but a violation of the entanglement bounds (dashed) is still found at large m. For all values of Γ, the QFI is calculated with respect to the rotation axis $\mathbf{n}$ that is optimal for $\Gamma = 0$.

the state overlap $F_t(\phi)$. However, for the parameters of Ref. [39], detecting entanglement should be feasible. The main source of decoherence in these experiments is off-resonant light scattering, which can be captured by including Lindblad terms in the master equation [45]. Specifically, we consider elastic Rayleigh scattering, which leads to coherence decay with rate Γ_{el}, and Raman scattering, i.e., incoherent transitions from $|\downarrow\rangle$ to $|\uparrow\rangle$ (Γ_{du}) and vice versa (Γ_{ud}). We emphasize that if $\Gamma_{du} = \Gamma_{ud}$, which is typically the case in the trapped-ion experiments, $\mathrm{tr}[\hat{\rho}_0\hat{\rho}_f] = \mathrm{tr}[\hat{\rho}_t\hat{W}(\phi)\hat{\rho}_t\hat{W}^\dagger(\phi)]$ in Eq. (1) still holds, and thus the I_m can still be detected using the time reversal scheme [45].

The role of decoherence is illustrated in Fig. 3, where the choice of parameters is motivated by the experimental capabilities demonstrated in Ref. [39]. Typical experimental parameters are $J \lesssim 5$ kHz, $t \lesssim 1$ ms, and a total decoherence rate $\Gamma \approx 60$ s^{-1}, dominated by Γ_{el}. Numerical simulations were performed using an efficient density matrix symmetrization approach [45].

Comparing $F_Q(\hat{\rho}_t, \hat{A})/N$ (black line) with the bound $F_I(\hat{\rho}_t, \hat{A})/N$ (red dashed), one recovers $F_Q(\hat{\rho}_t, \hat{A}) = F_I(\hat{\rho}_t, \hat{A})$ for pure states ($\Gamma = 0$), but as decoherence rates are increased, the bound quickly becomes less tight. While the QFI decays slowly at small Γt, the decay of the bound $F_I \sim e^{-N\Gamma t}$ is N-fold enhanced compared to the single-particle decay rate Γ because the global state overlap $\mathrm{tr}[\hat{\rho}_0\hat{\rho}_f]$ decays with this rate. The inverse spin-squeezing parameter [71], which also provides a lower bound on QFI, does not witness any entanglement for the case of Fig. 3(b), as the state is already strongly oversqueezed.

Figures 3(c) and 3(d) show the coherence spectra for two values of Γ. The main effect of dephasing is a global decay of the I_m with $e^{-N\Gamma t}$, approximately independent of m, as expected at short times in an initially pure system. Nevertheless, even for strong dephasing, the I_m still violate the entanglement bound for sufficiently large m, since the bound decreases exponentially with m, while the I_m decay much more slowly. Therefore, even in the presence of single-particle decoherence processes, we observe that the

I_m remain useful entanglement witnesses in the considered scenario. Nevertheless, one needs to deal with the experimental challenge of detecting a small signal, especially for large N. We note, however, that in Ref. [39], MQCs below 10^{-2} have been resolved.

In summary, we have derived inseparability criteria from the MQCs and a formal connection between MQCs and the QFI. Our results demonstrate that MQCs, a specific type of OTOCs, can serve as an experimentally accessible probe for detecting scrambling of quantum information and multiparticle entanglement in mixed states.

We thank Arghavan Safavi-Naini, Michael Wall, John Bollinger, Justin Bohnet, Graeme Smith, and Felix Leditzky for discussions. Supported by Defense Advanced Research Projects Agency (DARPA, W911NF-16-1-0576 through ARO), NSF Grant No. PHY 1521080, JILA-NSF Grant No. NSF-PFC-PHY-1734006, AFOSR-MURI, NIST, the DFG Collaborative Research Center SFB1225 (ISOQUANT), the Austrian Science Fund (FWF), through SFB FoQuS (No. F4016-N23), the ERC Synergy Grant UQUAM, and the ERC Advanced Grant EntangleGen (Project-ID 694561).

*Corresponding author.
martin.gaerttner@kip.uni-heidelberg.de

[1] E. Schrödinger, Math. Proc. Cambridge Philos. Soc. **31**, 555 (1935).
[2] L. D'Alessio, Y. Kafri, A. Polkovnikov, and M. Rigol, Adv. Phys. **65**, 239 (2016).
[3] A. M. Kaufman, M. E. Tai, A. Lukin, M. Rispoli, R. Schittko, P. M. Preiss, and M. Greiner, Science **353**, 794 (2016).
[4] C. Neill *et al.*, Nat. Phys. **12**, 1037 (2016).
[5] P. Hosur, X.-L. Qi, D. A. Roberts, and B. Yoshida, J. High Energy Phys. 02 (2016) 044.
[6] N. Y. Yao, F. Grusdt, B. Swingle, M. D. Lukin, D. M. Stamper-Kurn, J. E. Moore, and E. A. Demler, arXiv:1607.01801.
[7] B. Swingle, G. Bentsen, M. Schleier-Smith, and P. Hayden, Phys. Rev. A **94**, 040302 (2016).
[8] E. B. Rozenbaum, S. Ganeshan, and V. Galitski, Phys. Rev. Lett. **118**, 086801 (2017).
[9] G. Zhu, M. Hafezi, and T. Grover, Phys. Rev. A **94**, 062329 (2016).
[10] H. Shen, P. Zhang, R. Fan, and H. Zhai, Phys. Rev. B **96**, 054503 (2017).
[11] J. Li, R. Fan, H. Wang, B. Ye, B. Zeng, H. Zhai, X. Peng, and J. Du, Phys. Rev. X **7**, 031011 (2017).
[12] A. Bohrdt, C. Mendl, M. Endres, and M. Knap, New J. Phys. **19** 063001 (2017).
[13] B. Swingle and D. Chowdhury, Phys. Rev. B **95**, 060201 (2017).
[14] J. Maldacena, S. H. Shenker, and D. Stanford, J. High Energy Phys. 08 (2016) 106.
[15] Y. Sekino and L. Susskind, J. High Energy Phys. 10 (2008) 065.
[16] R. Fan, P. Zhang, H. Shen, and H. Zhai, Science Bulletin **62**, 707 (2017).
[17] J. Baum, M. Munowitz, A. N. Garroway, and A. Pines, J. Chem. Phys. **83**, 2015 (1985).
[18] P. Cappellaro, in *Quantum State Transfer and Network Engineering*, edited by G. M. Nikolopoulos and I. Jex, Quantum Science and Technology (Springer, Berlin, 2014) pp. 183–222.
[19] J. Baum and A. Pines, J. Am. Chem. Soc. **108**, 7447 (1986).
[20] M. Munowitz, A. Pines, and M. Mehring, J. Chem. Phys. **86**, 3172 (1987).
[21] C. M. Sánchez, R. H. Acosta, P. R. Levstein, H. M. Pastawski, and A. K. Chattah, Phys. Rev. A **90**, 042122 (2014).
[22] G. A. Álvarez and D. Suter, Phys. Rev. Lett. **104**, 230403 (2010).
[23] G. A. Álvarez, R. Kaiser, and D. Suter, Ann. Phys. (Amsterdam) **525**, 833 (2013).
[24] G. A. Álvarez, D. Suter, and R. Kaiser, Science **349**, 846 (2015).
[25] K. X. Wei, C. Ramanathan, and P. Cappellaro, arXiv: 1612.05249.
[26] S. I. Doronin, Phys. Rev. A **68**, 052306 (2003).
[27] G. B. Furman, V. M. Meerovich, and V. L. Sokolovsky, Phys. Rev. A **78**, 042301 (2008).
[28] G. B. Furman, V. M. Meerovich, and V. L. Sokolovsky, Quantum Inf. Process. **8**, 379 (2009).
[29] E. B. Fel'dman and A. N. Pyrkov, JETP Lett. **88**, 398 (2008).
[30] E. B. Fel'dman, A. N. Pyrkov, and A. I. Zenchuk, Phil. Trans. R. Soc. A **370**, 4690 (2012).
[31] G. Tóth and I. Apellaniz, J. Phys. A **47**, 424006 (2014).
[32] L. Pezzé, A. Smerzi, M. K. Oberthaler, R. Schmied, and P. Treutlein, arXiv:1609.01609.
[33] A. Widera, S. Trotzky, P. Cheinet, S. Fölling, F. Gerbier, I. Bloch, V. Gritsev, M. D. Lukin, and E. Demler, Phys. Rev. Lett. **100**, 140401 (2008).
[34] F. M. Cucchietti, J. Opt. Soc. Am. B **27**, A30 (2010).
[35] I. D. Leroux, M. H. Schleier-Smith, and V. Vuletić, Phys. Rev. Lett. **104**, 073602 (2010).
[36] J. S. Douglas, H. Habibian, C.-L. Hung, A. V. Gorshkov, H. J. Kimble, and D. E. Chang, Nat. Photonics **9**, 326 (2015).
[37] D. Linnemann, H. Strobel, W. Muessel, J. Schulz, R. J. Lewis-Swan, K. V. Kheruntsyan, and M. K. Oberthaler, Phys. Rev. Lett. **117**, 013001 (2016).
[38] T. Macrì, A. Smerzi, and L. Pezzè, Phys. Rev. A **94**, 010102 (2016).
[39] M. Gärttner, J. G. Bohnet, A. Safavi-Naini, M. L. Wall, J. J. Bollinger, and A. M. Rey, Nat. Phys. **13**, 781 (2017).
[40] W.-K. Rhim, A. Pines, and J. S. Waugh, Phys. Rev. Lett. **25**, 218 (1970).
[41] W.-K. Rhim, A. Pines, and J. S. Waugh, Phys. Rev. B **3**, 684 (1971).
[42] H. M. Pastawski, P. R. Levstein, G. Usaj, J. Raya, and J. Hirschinger, Physica (Amsterdam) **283A**, 166 (2000).
[43] P. R. Zangara, D. Bendersky, P. R. Levstein, and H. M. Pastawski, Phil. Trans. R. Soc. A **374**, 20150163 (2016).
[44] P. R. Zangara and H. M. Pastawski, Phys. Scr. **92**, 033001 (2017).

[45] See Supplemental Material at http://link.aps.org/supplemental/10.1103/PhysRevLett.120.040402 for details of proofs and numerical simulations, which includes Refs. [46–58].
[46] H. Uys, M. J. Biercuk, A. P. VanDevender, C. Ospelkaus, D. Meiser, R. Ozeri, and J. J. Bollinger, Phys. Rev. Lett. **105**, 200401 (2010).
[47] P. Schindler, D. Nigg, T. Monz, J. T. Barreiro, E. Martinez, S. X. Wang, S. Quint, M. F. Brandl, V. Nebendahl, C. F. Roos, M. Chwalla, M. Hennrich, and R. Blatt, New J. Phys. **15**, 123012 (2013).
[48] D. Girolami and B. Yadin, Entropy **19**, 124 (2017).
[49] R. Jozsa, J. Mod. Opt. **41**, 2315 (1994).
[50] J. Liu, H.-N. Xiong, F. Song, and X. Wang, Physica (Amsterdam) **410A**, 167 (2014).
[51] J. A. Miszczak, Z. P., P. Horodecki, A. Uhlmann, and K. Zyczkowski, Quantum Inf. Comput. **9**, 103 (2009).
[52] H. Kwon, C.-Y. Park, K. C. Tan, D. Ahn, and H. Jeong, arXiv:1704.06469 [Phys. Rev. A (to be published)].
[53] I. Marvian and R. W. Spekkens, Phys. Rev. A **94**, 052324 (2016).
[54] D. Girolami, Phys. Rev. Lett. **113**, 170401 (2014).
[55] T. Baumgratz, M. Cramer, and M. B. Plenio, Phys. Rev. Lett. **113**, 140401 (2014).
[56] S. Sarkar and J. S. Satchell, Europhys. Lett. **3**, 797 (1987).
[57] S. Hartmann, Quantum Inf. Comput. **16**, 1333 (2016).
[58] M. Xu, D. A. Tieri, and M. J. Holland, Phys. Rev. A **87**, 062101 (2013).
[59] While in NMR, the overlap measurement consists in measuring the magnetization $\sum_i \hat{\sigma}_i^z$; for pure states the projector $\bigotimes_i (1 - \hat{\sigma}_i^z)$ needs to be measured, which involves spin correlations of any order.
[60] This can be achieved easily for pure states and for strongly mixed states encountered in NMR experiments.
[61] S. L. Braunstein and C. M. Caves, Phys. Rev. Lett. **72**, 3439 (1994).
[62] L. Pezzé and A. Smerzi, Phys. Rev. Lett. **102**, 100401 (2009).
[63] P. Hyllus, W. Laskowski, R. Krischek, C. Schwemmer, W. Wieczorek, H. Weinfurter, L. Pezzé, and A. Smerzi, Phys. Rev. A **85**, 022321 (2012).
[64] G. Tóth, Phys. Rev. A **85**, 022322 (2012).
[65] B. Yadin and V. Vedral, Phys. Rev. A **93**, 022122 (2016).
[66] P. Hauke, M. Heyl, L. Tagliacozzo, and P. Zoller, Nat. Phys. **12**, 778 (2016).
[67] S. Pappalardi, A. Russomanno, A. Silva, and R. Fazio, J. Stat. Mech. (2017) 053104.
[68] For a general local operator $\hat{A} = \sum_j \mathbf{n}_j \cdot \hat{\mathbf{s}}_j$, we can just define the basis of the Hilbert space as a product of the eigenstates of the local spin operators $\mathbf{n}_j \cdot \hat{\mathbf{s}}_j$, which formally maps the problem to the case we consider explicitly.
[69] D. Leibfried, E. Knill, S. Seidelin, J. Britton, R. B. Blakestad, J. Chiaverini, D. B. Hume, W. M. Itano, J. D. Jost, C. Langer, R. Ozeri, R. Reichle, and D. J. Wineland, Nature (London) **438**, 639 (2005).
[70] J. G. Bohnet, B. C. Sawyer, J. W. Britton, M. L. Wall, A. M. Rey, M. Foss-Feig, and J. J. Bollinger, Science **352**, 1297 (2016).
[71] M. Kitagawa and M. Ueda, Phys. Rev. A **47**, 5138 (1993).